Journal of Supramolecular Structure 5:565 (417)–576 (428) (1976)

Measurement of the Lateral Mobility of Cell Surface Components in Single, Living Cells by Fluorescence Recovery After Photobleaching

K. Jacobson, Z. Derzko, E-S. Wu, Y. Hou, and G. Poste

Department of Experimental Pathology, Roswell Park Memorial Institute, Buffalo, New York 14263

The use of fluorescence recovery after photobleaching (FRAP) techniques to monitor the lateral mobility of plant lectin-receptor complexes on the surface of single, living mammalian cells is described in detail. FRAP measurements indicate that over 75% of the wheat germ agglutinin receptor (WGA-receptor) complexes on the surface of human embryo fibroblasts are mobile. These WGA-receptor complexes diffuse laterally (as opposed to flow) on the cell surface with a diffusion coefficient in the range of 2×10^{-11} to 2×10^{-10} cm^2/sec. Both the percentage of mobile WGA-receptor complexes and the mean diffusion coefficient of these complexes are higher than that obtained from earlier FRAP measurements of the mobility of concanavalin A-receptor (Con A-receptor) complexes in a variety of cell types. The possible reasons for the differing mobilities of WGA and Con A receptors are discussed.

Key words: **FRAP, lectins, wheat germ agglutinin, concanavalin A, lateral mobility, cell surface**

INTRODUCTION

Recent work in many laboratories has shown that lateral movement of membrane proteins, glycoproteins, and lipids can occur within the plane of the membrane (1–5) and that such transport may, in part, determine the functional properties of the cell surface (3–8). Prior to 1975, only a limited number of direct experimental measurements had been made on the transport of natural membrane proteins in situ. These experiments yielded lateral diffusion coefficients (D) ranging from about 5×10^{-9} cm^2/sec for

Abbreviations: FRAP, fluorescence recovery after photobleaching; D, diffusion coefficient; HEF, human embryo fibroblasts; F-WGA, fluorescein-conjugated wheat germ agglutinin; Con A, Concanavalin A; S-F-Con A, succinyl-fluorescein-Con A; FITC, fluorescein isothiocyanate; NAG, N-acetylglucosamine; PBS, phosphate-buffered saline.

E-S. Wu is now at the Department of Physics, University of Maryland-Baltimore County, Baltimore, MD 21228.

rhodopsin in photoreceptor membranes (9, 10) to less than 10^{-12} cm^2/sec for fluorescein-labeled surface proteins in the human erythrocyte (11). Within the last year, a number of further studies on single, cultured, mammalian cells have been reported. These recent results are based on the fluorescence recovery after photobleaching (FRAP) methodology first reported by Peters et al. (11). Experiments in which fluorescence-labeled concanavalin A (Con A) and its succinylated derivative were bound to mouse fibroblasts (12, 13) and rat myoblasts (14) have shown that the lateral mobility of the Con A-receptor complex can be characterized by a diffusion coefficient that ranges from $\sim 5 \times 10^{-11}$ cm^2/sec to $< 8 \times 10^{-12}$ cm^2/sec at 25°C. In myoblasts the apparent diffusion coefficient decreases with the concentration of lectin added to the cells and the total time the lectin resides on the cell surface, suggesting that time-dependent aggregation of the lectin receptor complexes is occurring (14). On the other hand, labeling of protein and lipid amino groups by fluorescein isothiocyanate (FITC), which presumably occurs without this complication of cross linking, has yielded diffusion coefficients of $(1-5) \times 10^{-10}$ cm^2/sec (15, 23).

In this report, we describe our progress in the development of FRAP methodology suitable for use with animal cells cultured in vitro and present new data on the lateral mobility of fluorescein-conjugated wheat germ agglutinin (F-WGA) bound to the surface of human embryo fibroblast cells.

METHODS

The FRAP Measurement: Concept and Definitions

The physical processes involved in the FRAP measurement are illustrated in Fig. 1. First, the emission (F_i) produced by a surface-specific fluorescence label on a small region of the cell surface is measured. Next, an intense, photobleaching pulse of light is directed

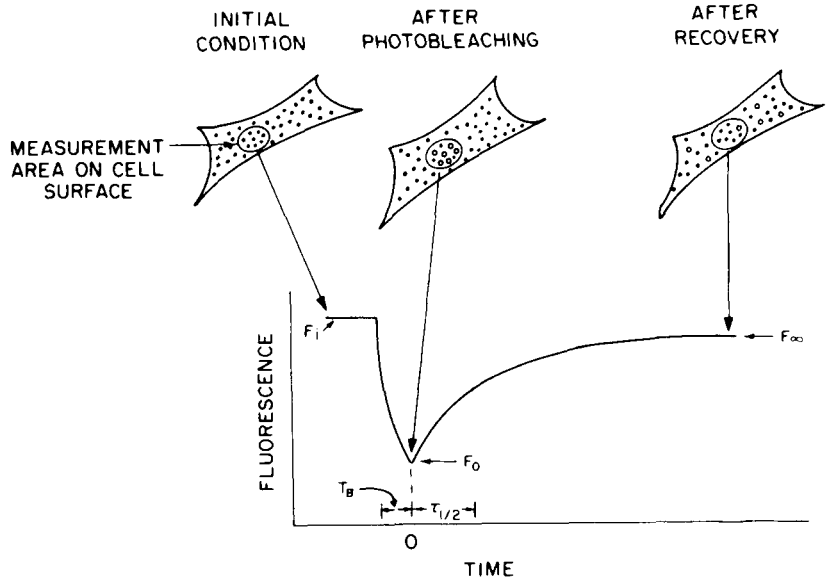

Fig. 1. Concept of the FRAP measurement of lateral transport of surface components of single, living cells. Unbleached fluorophores on cell surface are shown as closed dots (•), and the bleached fluorophores indicated as open circles (○). The area irradiated by laser is indicated by an oval outline on cell surface. Symbols (F_i,F_0,F_∞) for hypothetical FRAP data are defined in text.

to the same region of the cell surface for a time, T_B, which rapidly destroys a substantial amount of the fluorescence in that region. At the end of this photobleaching pulse, defined as time zero, the recovery of fluorescence within the photobleached region is measured as function of time with a beam coincident with the photobleaching beam and of the same intensity as that used to measure F_i. This fluorescence intensity ranges from F_0 at time zero to F_∞ at the time when the recovery is judged complete. Assuming that spontaneous recovery of fluorescence does not occur and that the probe beam does not itself induce photobleaching, the recovery kinetics must reflect the rate of lateral transport of neighboring unbleached fluorophores into the previously bleached region. The kinetics of recovery can be empirically characterized by the time ($\tau_{1/2}$) required to reach 50% of complete recovery; i.e., at $t = \tau_{1/2}$, $F = \frac{1}{2}(F_\infty - F_0) + F_0$. The percent recovery [$\%R \equiv (F_\infty - F_0)/(F_i - F_0)$] characterizes the extent to which the initial fluorescence (F_i) is regained. Fluorophores immobile on the time scale of the measurement are indicated by $\%R < 100\%$.

Instrumentation

A diagram of the fluorescence microscope used to perform FRAP measurements on cells in monolayer cultures is given in Fig. 2a and a photograph of the instrument is given in Fig. 2b. A 2 W argon laser (Model 551, Control Laser, Orlando, Fla.) is used to excite the fluorescence observed in a Leitz Ortholux II microscope equipped for incident light (Ploem) excitation. Eight lines spanning the spectral range of 458–515 nm are available using this laser, but use is generally restricted to the 488 or 496.5 nm line for FITC excitation. In the servo-looped mode the laser is stable to ± 1%. The laser beam is focused to a waist on the secondary image plane of the objective by a weak biconvex lens (FL; $f = 50$ cm). The objective further focuses the light to a 1.84 μ diameter ($1/e^2$ *width*) on the specimen (see below).

The laser, focusing lens, and a beam director (BD) (Newport Research Corp., Fountain Valley, Ca.) are all mounted on an optical bench behind and to the left of the microscope. The beam director changes the height and the direction of the beam by 90°,

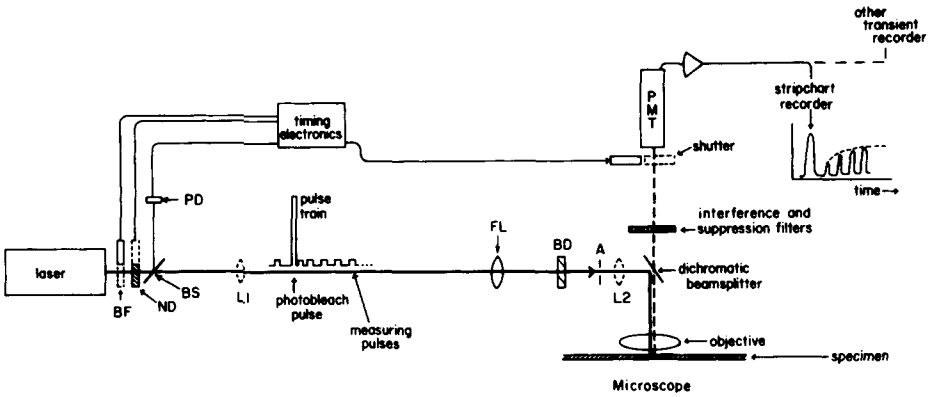

Fig. 2a. Diagram of the laser-excited fluorescence microscope used for FRAP measurements. BF, beam flag, ND, neutral density filter stack actuated by solenoid; BS, beam splitter; PD, photodiode used to trigger photomultiplier tube shutter; FL, focusing lens; BD, beam director; A, aperture; L1, L2, optional lenses to defocus laser beam; PMT, photomultiplier tube. The excitation beam path is indicated as a solid line; the path of detected fluorescence is indicated by the broken line.

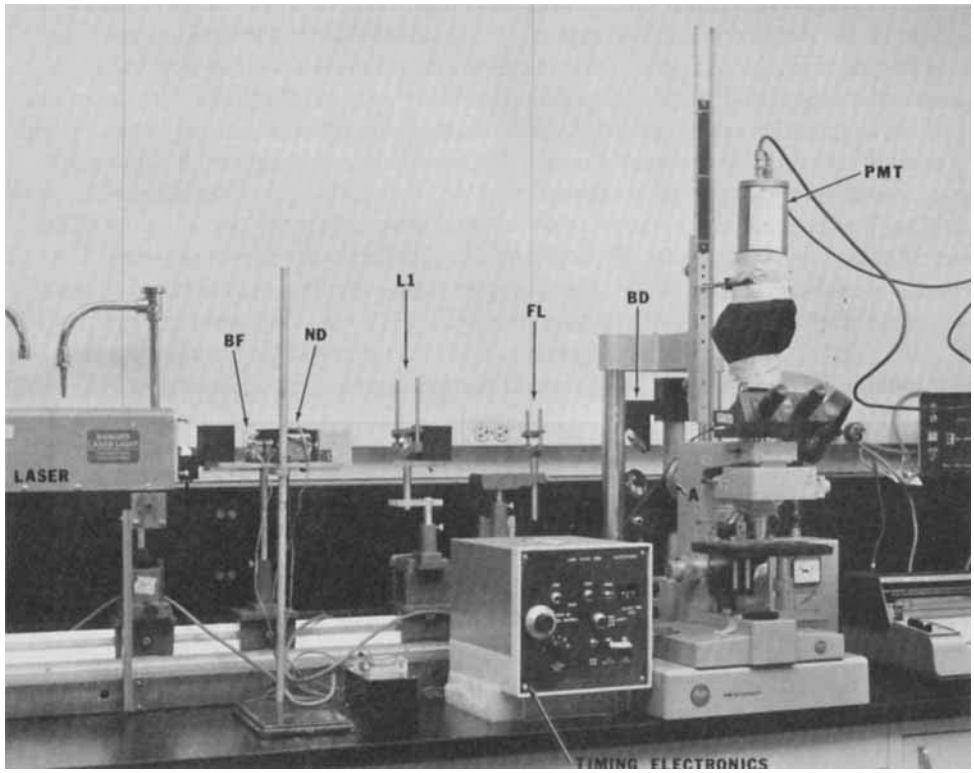

Fig. 2b. Photograph of the instrument described in Fig. 2a. The abbreviations are as in the legend to Fig. 2a.

allowing it to enter the microscope along the direction used by conventional incident excitation sources. The beam director is also used to center the beam in the field of view, and an iris diaphragm aperture (A) placed just behind the microscope stand serves to eliminate unwanted reflected beams. The field can be fully illuminated for conventional fluorescence microscopy by placing a strong biconvex lens (L1; f = 6.5 cm) in the beam and an unsymmetrical condenser (L2; f = 3.2 cm) just before the entrance aperture to the Ploem illuminator.

Fluorescence is measured through K530 suppression filters (Leitz, Rockleigh, N.J.) and a 530 nm (bandwidth ± 10 nm) interference filter (Corion Corp., Holliston, Mass.). The suppression filters are required to reduce breakthrough of the excitation light (496.5 nm), while the interference filters allow the green fluorescein emission to be isolated from the orange-yellow, granular autofluorescence produced by intracellular organelles. The photometer consists of an EMI 9789A photomultiplier tube driven by a stabilized high voltage supply (Model 150, SLM Instruments, Champaign, Ill.); the photocurrent is amplified by a picoamp preamplifier (Model 201, SLM Instruments, Champaign, Ill.) and its output is read on a stripchart recorder. The phototube is protected from unwanted illumination by an electronic camera shutter (Ealing Corp., South Natick, Mass.).

A beam flag (BF) just after the laser is actuated by a relay and controls when the specimen is illuminated. A neutral density filter (ND) to attenuate the beam for measure-

ment is driven by a solenoid. For a FRAP measurement these electromechanical devices are controlled by a digital electronic timing circuit (IC Electronics, Amherst, N.Y.) that allows precise definition of the duration of the photobleaching pulse (T_B) and the duration and interval between measurement pulses [the measuring beam is not left on continuously, in order to avoid possible photobleaching during the recovery phase of the experiment (12, 14)] ; in addition, the shutter in front of the phototube is triggered to the open position by a photodiode (PD) that senses the fall in the laser intensity at the end of the photobleaching pulse. This feature protects the phototube from the intense photobleaching pulse.

In a typical experiment, F_i is first measured manually by switching the phototube shutter to open and the neutral density filters into the beam. Following this, the beam stop is switched out of the beam and the initial fluorescence (F_i) recorded. The rest of the measurement is automated and actuated by a start button on the electronic timing module. First, photobleaching occurs for a preset time (10 msec $< T_B <$ 10 sec), followed by measurement pulses starting at time zero and continuing at intervals (T_{off}) that can vary from 1 to 32 sec, and with pulse durations (T_{on}) of 0.5 sec to 5 sec. The accuracy of short bleaching pulses and the definition of time zero depend on the speed of the electromechanical devices actuating the beam flag and neutral density filter.

The size of the focused beam in the plane of the specimen is a critical parameter for FRAP measurements yet is difficult to measure or calculate accurately. For the purposes of this report, the approximate beam diameter has been calculated by the following procedure. The weak focusing lens is positioned to produce a waist on the secondary image plane of the microscope, which is conjugate to the in-focus specimen plane. The $1/e^2$ radius of this waist (w_1) can be calculated from the waist-waist transformation law (see, for example, 16):

$$1/w_1^2 = (1/w_0^2)\,(1-d_1/f)^2 + (1/f^2)\,(\pi w_0/\lambda)^2 \qquad (1)$$

where, w_0 is the $1/e^2$ radius of the laser waist, d_1 is the distance of this waist from lens FL, f is the focal length of FL, and λ is the laser wavelength. The position of the waist within the laser depends on its design. For our laser, w_0 was calculated to be 0.691 mm and the waist is positioned at the rear, plane mirror resulting in a value for d_1 of 168 cm.

The distance d_1' of the waist created by lens FL from this lens is given by (16):

$$(d_1'-f) = (d_1-f)\,f^2/[(d_1-f)^2 + (\pi w_0^2/\lambda)^2] \qquad (2)$$

This gives the approximate distance away from the secondary image plane to put the focusing lens. For our experiment, w_1 = 0.107 mm and d_1' = 52.8 cm.

A second application of the waist-waist transformation (Equation 1) for the microscope objective (× 100; f = 1.7 mm) gives a spot size ($2w_s$, the $1/e^2$ diameter) in the specimen plane of 1.84 μ. This we take to be our nominal beam diameter, and a recent report shows that measured diameters of micron size beams produced by microscope objectives can be predicted by theory at least down to the 2 μ region (17). It should be noted that the well-known relation between object and image size from geometrical optics (magnification = image size/object size) gives a similar spot size (2.14 μ).

Scanning the beam in the specimen plane can be accomplished to directly give the beam diameter, though this is a difficult measurement. Scanning the expanded beam

below the waist generated by the objective can give the beam diameter at the waist, provided the law of expansion holds (16):

$$w_z = w_s [1 + (\lambda z/\pi w_s^2)^2]^{1/2} \quad (3)$$

where w_z is the expanded beam radius at distance z from the location of the waist (of radius w_s) produced by the objective.

Recently Axelrod et al. (18) have pointed out that beam size measurements can be obtained by a flow calibration procedure. This may prove very helpful, as we have noticed that the profile of the laser beam is not always perfectly Gaussian. The various asymmetries in the profile seem to depend on the wavelength of operation as well as the laser power level. It is possible that occasionally modes other than Tem_{00} are contributing to the beam. We are presently exploring means to experimentally characterize the beam profile and diameter. We have found the 496.5 nm line at 100 mW gives an approximately Gaussian spatial profile by scanning the expanded beam with a photodiode below the waist created by the objective. The experiments described in this report were performed under these conditions.

Additional Considerations for Operation

Cells grown on glass coverslips (see below) are located using a dark field condenser with tungsten illumination filtered by a Corning CS-67 colored glass filter to prevent possible photobleaching during the location procedure. When this image was sharply focused, it was found that the surface fluorescence was also in focus. However, it should be noted that photobleaching and recovery will also occur on the bottom surface of the cell, assuming this surface is also labeled with the lectin. Hence, an average recovery will be obtained from the two surfaces. An additional complication is that the out-of-focus surface will be bleached under different conditions than the in-focus surface, namely that, because the beam expands from its waist approximately according to Equation 3, a larger area will be bleached on the out-of-focus surface compared to the in-focus surface. Bleaching time was less than $\tau_{1/2}/10$ and the bleaching power was in the 1 mW range. The measuring power was fixed to allow no more than 3% fading during an experiment with noise levels $\sim \pm 5\%$ of signal. Typical measuring power levels were in the 10–100 nW range.

Because of the variety of difficult systematic errors in the measurement, more emphasis has been placed on obtaining reproducible results so that different biological situations can be compared rather than on the absolute accuracy of lateral transport rates for membrane components calculated from the FRAP data.

Data Analysis

The most elementary form of analysis is to calculate $\tau_{1/2}$ and %R for a given recovery curve. To obtain lateral transport rates from these data demands assumption of a given model of transport on the cell surface. Basically, this requires solution of the transport differential equation subject to the initial condition created by photobleaching. Diffusional models that assume an initial condition created by photobleaching have been given earlier for an infinite plane surface (12) and a spherical surface (19). A complete treatment for the infinite plane surface in which the initial condition created by photobleaching is calculated for both Gaussian and circular beams has been presented recently by Axelrod et al. (18). In this theoretical study, the recovery curves for diffusion, uniform flow, and

mixed modes occurring in a flat plane have been computed and methods for data analysis given. This analysis will be applied to the experimental results presented below.

In brief, the initial condition is created by an intense, focused laser beam impinging on a uniform, two-dimensional concentration of fluorophores. If these fluorophores are assumed to photobleach with irreversible, first-order kinetics, the photobleaching can be characterized by a parameter, K:

$$K \equiv \alpha T_B I(0) \tag{4}$$

where α is a factor in the first-order rate constant, T_B is the duration of the photobleaching pulse, and I(0) is the intensity of the laser beam at its center. The TEM_{00} mode of a laser has a Gaussian spatial profile of intensity:

$$I(r) = (2P_0/\pi w_s^2) \exp(-2r^2/w_s^2) \tag{5}$$

where, P_0 is the total laser power, w_s is the $1/e^2$ radius of the beam at the specimen plane and r is the distance in a plane normal to the beam direction and measured outward from the beam center along a radius. The parameter K can be determined from the experimental ratio of F_0/F_i according to the relation:

$$F_0/F_i = K^{-1}(1 - e^{-K}) \tag{6}$$

The recovery kinetics can then be calculated by solving the appropriate differential equation of lateral transport subject to the initial condition created by photobleaching and characterized by K.

Axelrod et al. (18) have plotted a number of these K-dependent curves for diffusion, uniform flow, and mixed cases and they outline curve-fitting procedures. For example, in a FRAP measurement using a Gaussian bleaching beam, for diffusive lateral transport the diffusion coefficient (D) is given by:

$$D = (w_s^2/4\tau_{1/2})\gamma_D \tag{7}$$

where, γ_D is a function of K (18). This procedure requires knowledge of F_∞ in order that $\tau_{1/2}$ can be computed. γ_D varies from about 1.1 to 1.45 for $0 < K < 5.0$; i.e., bleaching is restricted to $F_0/F_i > 20\%$. Our previous calculation (12) to obtain a diffusion constant from FRAP kinetics is equivalent to taking $\gamma_D = 1.28$. Practically, this means that diffusion constants obtained from our calculations will agree to within ± 15% of the result obtained using the theory of Axelrod et al. (18) for $K < 5$. This agreement indicates that for moderate photobleaching the calculated diffusion constant is not exceptionally sensitive to the choice of initial condition. A method involving superposition of experimental and theoretical curves on log-log paper that does not require an estimate of F_∞ has also been given by Axelrod et al. (18).

It should be noted that the degree to which any model is applicable to the analysis of the data depends on how well the experimental conditions match the assumptions of the theory. For example: Is photobleaching an irreversible, first-order process? How important is an exact Gaussian beam profile? To what degree do actual lateral transport processes depart from the simple theoretical processes, which allow convenient solution?

Cells and Reagents

A strain of human embryo fibroblasts (HEF) derived from fetal foreskin was obtained from Dr. Eric Mayhew and cultured in monolayer using Dulbecco's modified Eagle's medium with 10% fetal calf serum (Gibco, Grand Island, N. Y.). The cells used in this study were in their 15th to 26th passage.

Wheat germ agglutinin (WGA), isolated and purified as described by LeVine et al. (20), was kindly provided by Dr. Howard Allen, and showed a single band upon SDS-polyacrylamide gel electrophoresis. Fluorescein isothiocyanate (FITC; Sigma, St. Louis, Mo.) was conjugated to WGA by standard methods (21) except that, to protect the binding site, the haptenic inhibitor N-acetylglucosamine (NAG; Sigma, St. Louis, Mo.) was added to the reaction mixture at a concentration of 10 mM. Protein concentrations and dye-to-protein ratio were determined spectrophotometrically. About 0.66 dye molecules were conjugated to each WGA. Concanavalin A-sepharose was obtained from Pharmacia (Piscataway, N. J.) and conjugated to FITC as above.

Coverslip cell cultures were labeled at 25° by first washing three times in phosphate-buffered saline (PBS), then incubating for 2 min with 1 ml of 1–26 μg/ml F-WGA in PBS, and then washing three times with PBS. The coverslips were then wet-mounted on microscope slides and sealed with a molten paraffin-vasoline mixture for study.

RESULTS AND DISCUSSION

Control Studies

One important assumption involved in the FRAP method is that spontaneous recovery of fluorescene from the fluorophores in the photobleached region is negligible. In order to establish the validity of this assumption, measurements were made on FITC-conjugates of Con A-sepharose beads. In this system, the fluorescein moieties should be completely immobilized with respect to submicron translational movements so that following photobleaching any recovery of fluorescence must have resulted from spontaneous chemical recovery. As shown in Fig. 3, no detectable recovery is observed, indicating the absence of spontaneous fluorescence recovery for FITC.

Single-cell fluorescence measurements of the relative amounts of F-WGA bound to HEF cells in the presence and absence of the haptenic inhibitor N-acetylglucosamine (NAG) revealed that the average intensity for 11 cells incubated with 2.6 μg/ml F-WGA for 5 min was 33.9 ($\sigma = \pm 3.7$) arbitrary units, whereas the same incubation in the presence

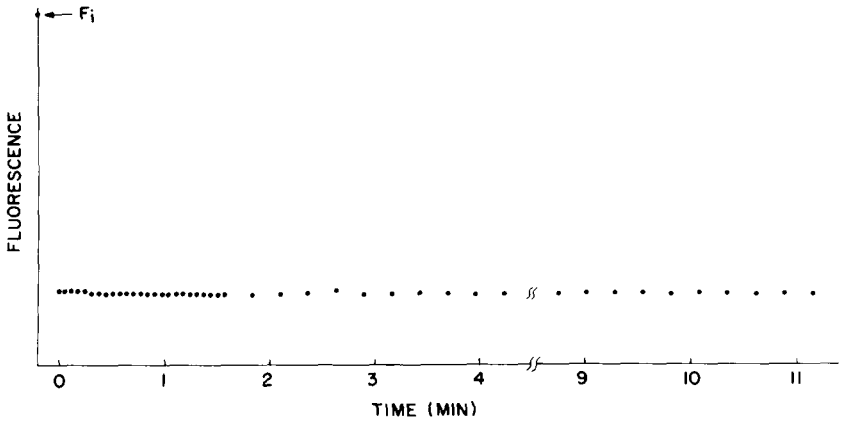

Fig. 3. FRAP results at 25° for FITC-conjugated Con A-sepharose beads. Bleaching power 2.5 mW at 488 nm; T_B = 550 msec. Bleaching beam attenuated by 10^5 for measuring. × 53 objective employed.

of 100 mM NAG gave an average intensity (10 cells) of 3.5 ($\sigma = \pm 0.4$). The residual 10% fluorescence in the presence of the inhibitor may represent "nonspecific" lectin binding or it may indicate the presence of a small number of high-affinity binding sites.

Mobility Studies

In a previous publication (12), we demonstrated that the FRAP method could be used to measure diffusion of the macromolecule, succinyl-fluorescein-Con A (S-F-Con A) dissolved in glycerol saline solutions. Figure 4 shows the recovery kinetics for this experiment. The curve in Fig. 4 is plotted according to a simple theoretical model given earlier (12), which is adjusted to fit the data by varying the parameter D. The best fit for this data is obtained by employing $D = 7.4 \times 10^{-10}$ cm^2/sec. By comparison, the theory of Axelrod et al. (18) can be fitted to our data by employing a $D = 6.7 \times 10^{-10}$ cm^2/sec. Calculation of the diffusion coefficient of S-F-Con A in 98% glycerol using the Stokes-Einstein equation, with due regard to the assumptions underlying its application, gives a value of 7×10^{-10} cm^2/sec. The agreement of these results strongly suggests that, in this case, FRAP kinetics are diffusion-controlled. Subsequently, Axelrod et al. (18) showed that the FRAP kinetics of aqueous rhodamine 6G could be fitted with their theoretical model by employing diffusion coefficients of the expected magnitude.

FRAP kinetics at 25° are given in Fig. 5 for HEF cells labeled with 10 μg/ml F-WGA for 2 min. This datum is from the second photobleaching on the same spot, and recovery is seen to be very nearly 100%. In the first photobleaching, the kinetics were similar and the %R was about 85%. The thin solid line is calculated from the theory of Axelrod et al.

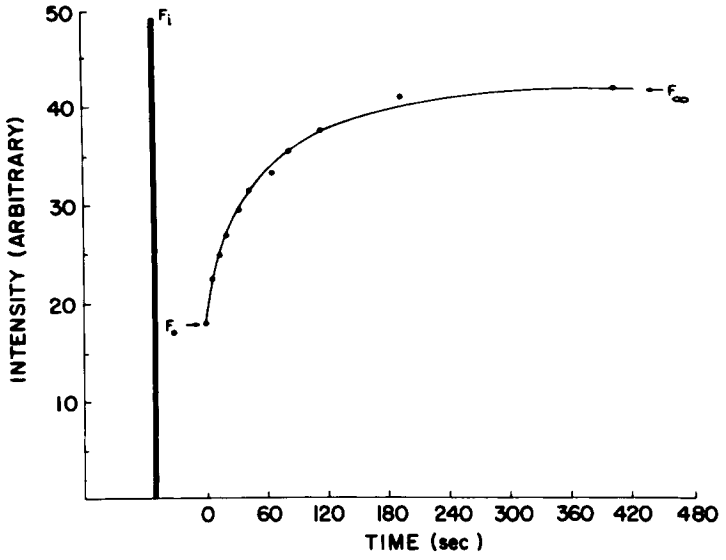

Fig. 4. Recovery kinetics of 2 μM S-F-Con A in 98% glycerol-2% PBS (v/v) at 22°C. Points represent experimental data with F_i denoted by the broad bar to the left of the origin. The plotted line is the theoretical curve obtained from Equation 2 (Ref. 12) using $D = 7.4 \times 10^{-10}$ cm^2/sec and $a = 2.9$ μ; F_∞ was chosen as 41.5 units and experimental values are indicated by the symbols. X 20 objective was employed and photobleaching beam was attenuated by 20,000 for measuring. This figure is reproduced from Jacobson et al. (1976), Biochim. Biophys. Acta 433:215, with permission of ASP Biological and Medical Press, Amsterdam.

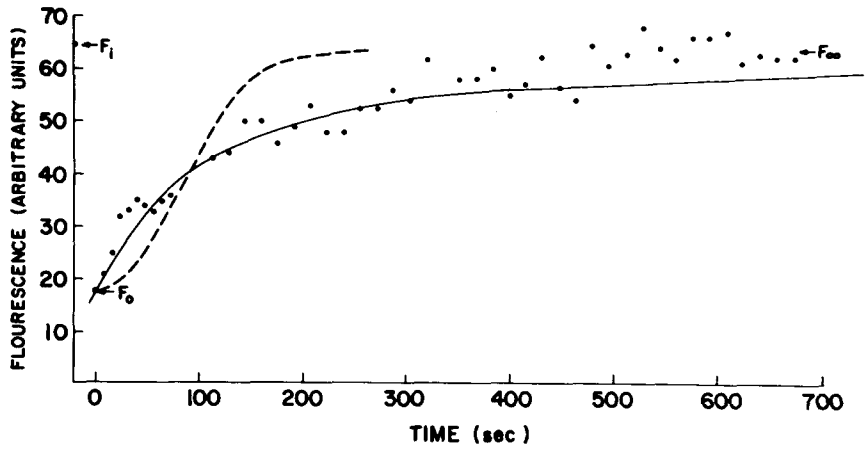

Fig. 5. FRAP results at 25° for nonconfluent HEF cells (passage 24) labeled for 2 min with 10 μg/ml F-WGA; second photobleaching. The measurement was made 20 min after lectin was added to the monolayer. Bleaching power: 2.5 mW at 496.5 nm; T_B = 350 msec. The bleaching beam was attenuated by 31,623 (neutral density 4.5) for the measurement and a × 100 objective employed. The thin solid line represents the theoretical fit (see Ref. 18) for D = 3.1 × 10^{-11} cm^2/sec, and the broken line shows the fit for simple one-directional flow of velocity of about 0.01 μ/sec.

(18) for purely diffusional recovery with D = 3.1 × 10^{-11} cm^2/sec. The broken line represents a simple, unidirectional flow recovery with a velocity of about 0.6 μ/min. Comparison of these two theoretical curves indicates that the observed recovery is much more easily interpreted as diffusion-controlled rather than flow-controlled. It should be noted that the recovery data exhibit considerable "noise." It is possible that some of this "noise" is due to structural fluctuations on the cell periphery such as microvillus formation and retraction and extension of larger ruffles and lamellae. The noticeable undershoot of the theoretical diffusion curve (Fig. 5; 400 sec < t < 600 sec) at long times may be caused by sudden transport of F-WGA-receptor complexes into the measurement area by processes not connected with the diffusional recovery. Similarly, a "wavering" component modulating the FRAP curves for rhodamine-Con A bound to myoblasts was reported earlier (14).

At this stage in the application of FRAP measurements to living cells certain semi-quantitative trends are emerging.

For the HEF cells examined in this study, the %R was almost always greater than 60%; in a series of 28 measurements employing F-WGA concentrations of 2.6–26 μg/ml the mean %R was 80% (σ = ± 2.6%). There were no pronounced trends in %R as the F-WGA incubation concentration was varied from 2.6 to 26 μg/ml and as the time that the lectin resided on the cell surface ranged from 10 to 100 min. These %R values are higher than those previously obtained in FRAP measurements of Con A binding to mouse fibroblasts (12, 13) and rat myoblasts (14). Almost invariably, the %R figure for the second of two successive photobleachings on the same spot was higher than the first, in agreement with earlier experiments (14). This result is expected if immobilized fluorophores are preferentially removed from the measurement in successive FRAP experiments.

The diffusion constants for WGA-receptor complexes estimated from the fit of theory to experiment (18) were in the range of 2 × 10^{-11} to 2 × 10^{-10} with most values

above $D = 8 \times 10^{-11}$ cm^2/sec. These values are about an order of magnitude greater than those reported earlier for Con A diffusion on the surfaces of myoblasts (14), though as pointed out above, such comparisons are sensitive to systematic errors in each particular instrument. Furthermore, no pronounced variations of $\tau_{1/2}$ with the "residence" time of the lectin on the cell surface or with incubation concentration occurred again in contrast to earlier studies with Con A (13, 14).

It thus appears that the class(es) of WGA-receptor complexes in HEF cells examined in this study are somewhat more mobile than the Con A-receptor complexes in myoblasts and fibroblasts derived from rodents, both in terms of the apparent diffusion coefficient of the lectin-receptor complex and the degree to which these receptors are "anchored." This apparent largely "unanchored" state of the WGA receptors is consistent with other observations that suggest that WGA receptors, in contrast to Con A receptors, are not linked to membrane-associated cytoskeletal elements on the inner face of the plasma membrane (4, 8, 22). A further possibility is that the relatively large D and high %R observed for the F-WGA-receptor complex could result from the fact that a substantial proportion of the WGA receptors are situated on glycolipids.

The lack of a pronounced dependence of %R and $\tau_{1/2}$ on either the residence time of the F-WGA on the cell surface or the lectin incubation concentration argues against substantial aggregation of the lectin-receptor complexes during the experiment but does not preclude a fast aggregation reaction, which is substantially completed before the measurement begins. Because of this possibility, we cannot make a definite conclusion about possible differences in the intrinsic mean mobilities of WGA and Con A receptors. However, the fact that most of the diffusion constants determined from FRAP curves for the F-WGA-receptor complexes approach the values ($1 \times 10^{-10} < D < 3 \times 10^{-10}$ cm^2/sec) obtained by methods designed to label integral membrane proteins (14, 15, and Schlessinger et al., in preparation) suggests that F-WGA-receptor complexes may be small, even dimeric, aggregates.

The results reported here, and in previous publications (12–15), indicate that the FRAP technique provides a useful tool for studying the lateral mobility of components located on the cell periphery.

ACKNOWLEDGMENTS

We thank Drs. Howard Allen and Eric Mayhew for gifts of wheat germ agglutinin and cells, respectively, and for several helpful discussions. We also thank members of the Biophysics Group at Cornell University for many useful discussions. We thank Dr. Darold Wobschall of IC Electronics, Amherst, N.Y., for his special design of our digital timing circuitry. We acknowledge the support of N.I.H. grants CA 16743 (K. J.) and CA 13393 (G. P.).

REFERENCES

1. Edidin, M.: Ann. Rev. Biophys. Bioengin., 3:179 (1974).
2. Nicolson, G. L.: Int. Rev. Cyt., 39:89 (1974).
3. Nicolson, G. L., and Poste, G.: New Eng. J. Med., 295: 197 and 253 (1976).
4. Edelman, G. M.: Science, 192:218 (1976).
5. Bretcher, M., and Raff, M.: Nature, 258:43 (1975).
6. Ukena, T. E., Borysenko, J. Z., Karnovsky, M. J., and Berlin, R. D.: J. Cell Biol., 61:70 (1974).

7. DePetris, S.: J. Cell Biol., 65:123 (1975).
8. Poste, G., Papahadjopoulos, D., Jacobson, K., and Vail, W.: Biochim. Biophys. Acta, 394:520 (1975).
9. Poo, M. M. and Cone, R.: Nature, 247:438 (1974).
10. Liebman, P., and Entine, G.: Science, 185:457 (1974).
11. Peters, R., Peters, J., Tews, K., and Bahr, W.: Biochim. Biophys. Acta, 367:282 (1974).
12. Jacobson, K., Wu, E-S., and Poste, G.: Biochim. Biophys. Acta, 433:215 (1976).
13. Zagyansky, Y., and Edidin, M.: Biochim. Biophys. Acta, 433:209 (1976).
14. Schlessinger, J., Koppel, D., Axelrod, D., Jacobson, K., Webb, W., and Elson, E.: Proc. Nat. Acad. Sci. USA, 73:2409 (1976).
15. Edidin, M., Zagyanski, Y., and Lardner, T.: Science, 191:466 (1976).
16. Dickson, L.: Applied Optics, 9:1854 (1970).
17. Suzaki, Y., and Tachibana, A.: Applied Optics 14:2809 (1975).
18. Axelrod, D., Koppel, D., Schlessinger, J., Elson, E., and Webb, W.: Biophys. J., 16:1055 (1976).
19. Lardner, T., and Solomon, N.: J. Theoret. Biol. 60:433 (1976).
20. LeVine, D., Kaplan, M., and Greenaway, P.: Biochem. J., 129;847 (1972).
21. Wood, B., Thompson, S., and Goldstein, G.: J. Immunol., 95:225 (1965).
22. Poste, G., Papahadjopoulos, D., and Nicolson, G. L.: Proc. Nat. Acad. Sci. U.S.A., 72:4430 (1976).
23. Schlessinger, J., Axelrod, D., Koppel, D., Webb, W. and Elson, E.: Science, 195:307 (1977).